Journal of Pharmaceutical and Biomedical Analysis 50 (2009) 432–439

Contents lists available at ScienceDirect

Journal of Pharmaceutical and Biomedical Analysis

journal homepage: www.elsevier.com/locate/jpba

# Quinoline alkaloids in honey: Further analytical (HPLC-DAD-ESI-MS, multidimensional diffusion-ordered NMR spectroscopy), theoretical and chemometric studies

Giangiacomo Beretta[a,*], Roberto Artali[a], Enrico Caneva[b], Serena Orlandini[c], Marisanna Centini[d], Roberto Maffei Facino[a]

[a] Department of Pharmaceutical Sciences "Pietro Pratesi", Faculty of Pharmacy, University of Milan, via Mangiagalli 25, 20133 Milan, Italy
[b] CIGA-Centro Interdipartimentale Grandi Apparecchiature, University of Milan, via Golgi 19, 20133 Milan, Italy
[c] Department of Pharmaceutical Sciences, Faculty of Pharmacy, University of Florence, Via U. Schiff 6, Sesto Fiorentino, 50019 Florence, Italy
[d] Centro Interdipartimentale di Scienza e Tecnologia Cosmetiche, University of Siena, Via della Diana 2, 53100 Siena, Italy

ARTICLE INFO

*Article history:*
Received 23 April 2009
Accepted 25 May 2009
Available online 6 June 2009

*Keywords:*
Honey
Pyrrolidinyl quinoline alkaloids
Kynurenic acid
Nuclear magnetic resonance
High pressure liquid chromatography
Mass spectrometry

ABSTRACT

The wound-healing properties of honey are well established and it has been suggested that, among its pharmaco-active constituents, kynurenic acid (KA) exerts antinociceptive action on injured tissue by antagonizing NMDA at peripheral GABA receptors. The aim of this study was to investigate the quantitative profile of KA and of two recently identified, structurally related derivatives, 3-pyrrolidinyl-kynurenic acid (3-PKA) and its γ-lactamic derivative (γ-LACT-3-PKA), by examining their mass spectrometric behavior, in honeys from different botanical sources. We used a combination of HPLC-DAD-ESI-MS and NMR techniques (one-dimensional $^1$H NMR and diffusion-ordered spectroscopy NMR).

Chestnut honey constantly contained KA (2114.9–23 g/kg), 3-PKA (482.8–80 mg/kg) and γ-LACT-3-PKA (845.8–32 mg/kg), confirming their reliability as markers of origin. A new metabolite, 4-quinolone (4-QUIN), was identified for the first time in one chestnut honey sample (743.4 mg/kg). Small amounts of KA were found in honeydew, sunflower, multifloral, almond and eucalyptus honeys, in the range of 23.1–143 mg/kg, suggesting contamination with chestnut honey. Total phenol content (TPC) was in the range from 194.9 to 1636.3 $mg_{GAE}$/kg and total antiradical activity (TAA) from 61 to 940 $mg/_{GAE}$/kg), depending on the botanical origin.

Principal component analysis (PCA) was then done on these data. The three different clusters depicted: (i) antinociceptive activity from KA and/or its derivatives, typical of chestnut honey; (ii) antioxidant/radical scavenging activity by antioxidants responsible for the antiinflammatory action (dark honeys); (iii) peroxide-dependent antibacterial activity due to $H_2O_2$ production by glucose oxidase in honey.

The PCA findings provide useful indications for the dermatologist for the treatment of topical diseases, and the profiling of KA and its derivatives may shed light on new aspects of the kynurenine pathway involved in tryptophan metabolism.



## 1. Introduction

Kynurenic acid (KA) is a tryptophan metabolite formed through the kynurenine pathway and is considered ubiquitous in living systems. Since its discovery in dog urine in 1853 [1], it has been found in the central nervous system of mammals [2] and insects [3], in plants [4], and in biological fluids and organs [5,6]. It has recently been detected in edible vegetables, meat, and honeybee products, arousing even more interest in its biochemistry and biological functions [7,8].

KA (Fig. 1) is the only known endogenous antagonist of all subtypes of ionotropic glutamate receptors [9]. It is preferentially active not only at the glycine allosteric site of the N-methyl-D-aspartate (NMDA) receptor, but also acts as a non-competitive antagonist of α7 nicotinic acetylcholine receptors (AR) and mediates α-amino-3-hydroxy-5 methyl-4-isoxazole propionic acid (AMPA) receptor responses [10].

We have already identified KA in honey from different botanical origins through a combination of spectrometric techniques (multidimensional NMR and high-resolution mass spectrometry—HRMS),

*Abbreviations:* KA, kynurenic acid; 3-PKA, 3-(2′-pyrrolidinyl)-kynurenic acid γ-LACT-3-PKA; TPC, total phenol content; ARA, antiradical activity; IDO, indoleamine-2,3-dioxygenase; GAE, gallic acid equivalent; DOSY, dispersion ordered spectroscopy; HPLC, high pressure liquid chromatography; NMR, nuclear magnetic resonance; MS, mass spectrometry; SIM, single ion monitoring.

* Corresponding author. Tel.: +39 02 503 19317; fax: +39 02 503 19359.
*E-mail address:* giangiacomo.beretta@unimi.it (G. Beretta).

0731-7085/$ – see front matter © 2009 Elsevier B.V. All rights reserved.
doi:10.1016/j.jpba.2009.05.029

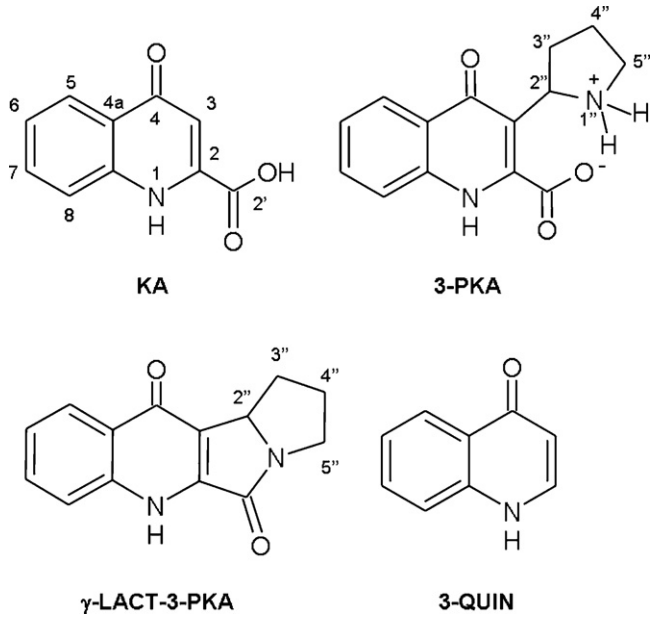


**Fig. 1.** Chemical structure of the quinoline alkaloids identified by HPLC-DAD, HPLC–MS and dispersion ordered spectroscopy (DOSY) NMR in chestnut honey: kynurenic acid (KA), 3-pyrrolidinyl kynurenic acid (3-PKA), the γ-lactam derivative of 3-PKA (γ-LACT-3-PKA) and 4-quinolon (3-QUIN).

with the highest content in chestnut honey. More recently we found two new KA derivatives in the same honey, which we studied by a multidimensional NMR approach [11]. This led us to propose for the first of these, 3-PKA, a pyrrolidinyl moiety at the C-3 of KA, and for the second the structure of the γ-lactam derivative of 3-PKA, γ-LACT-PKA, arising from intramolecular condensation between the C2 carboxyl moiety of KA and the aminic nitrogen of the pyrrolidinyl side chain (Fig. 1). However, no MS study of these derivatives has been reported.

Interest in the use of honey as a skin dressing for the treatment of wounds and burns in clinical practice [12] is based on: (i) its peroxide-dependent antibacterial activity; (ii) the presence of an array of specific antiinflammatory constituents; (iii) the possibility that KA might have antinociceptive action on injured tissue by antagonizing NMDA at peripheral GABA receptors [8,13,14].

The aims of this work were therefore: (i) to investigate the quantitative profile of KA, 3-PKA and γ-LACT-3-PKA (after theoretical assessment of their ability to bind at the glycine allosteric site of the NMDA receptor), in honeys from different botanical sources, and of the newly discovered derivative of KA, 4-quinolone (4-QUIN); (ii) to evaluate the total phenol content (TPC) and total antiradical activity (TAA) of different honeys. Honey components among which phenolic acids, flavonoids, Maillard products, carotenoids are involved in attenuation of the inflammatory process since they participate in COX-1 and COX-2 inhibition, in scavenging ROS and free radicals, and in the action of inflammatory mediators (cytokines) [15]; (iii) to apply a standard chemometric approach (principal component analysis, PCA) to predict the potential antinociceptive and antiinflammatory activity.

The results provide information that might help explain the therapeutic properties of honeys from floral or arboreal sources, and assist the dermatologist in deciding the most appropriate type of honey for clinical use. In addition they shed light on an interesting connection between KA and its derivatives 3-PKA, γ-LACT-3-PKA and 4-QUIN which could open up new metabolic perspectives on KA turnover in honeybees, mediated by the kynurenine pathway.

## 2. Material and methods

### 2.1. Chemicals

All chemicals, reagents and KA were of analytical grade, purchased from Sigma-Fluka-Aldrich Chemical Co. (Milan, Italy). HPLC-grade, analytical-grade organic solvents and deuterated dimethylsulphoxide (DMSO-$d^6$) were also purchased from Sigma-Fluka-Aldrich (Milan, Italy). HPLC-grade water was prepared with a Milli-Q water purification system (Millipore, Bedford, MA, USA).

### 2.2. Honey samples

Commercial honey samples were purchased from local stores or from beekeepers in the region around Milan, authenticated and processed with the procedures previously described [16].

### 2.3. Sample preparation and calibration curves

Samples for HPLC-DAD-ESI-MS and diffusion-ordered spectroscopy (DOSY) NMR were prepared as previously reported [8,17]. Ten grams of honey were diluted to 100 mL with distilled water, stirred until completely dissolved, filtered through cotton to remove solid particles, and the pH was adjusted to 2.5 with 6N HCl. The filtrate was passed through a RP-SPE cartridge filled with solid phase (3 g of silica-bonded C-18 resin, Discovery® DSC-18, Supelco, Bellefonte, PA, USA), and after washing first with acidic water (HCl, 50 mL, pH 3) then with neutral water (50 mL), the substances retained in the column were recovered by elution with methanol (20 mL). The methanol fraction was dried under a gentle stream of nitrogen, and the residue was taken up in 600 μL of DMSO-$d^6$ for NMR analysis or with a 7:3 $H_2O$/acetonitrile mixture for HPLC–MS.

Samples for HPLC analysis were prepared by diluting 1 g of honey with 1 mL of acidic water ($CF_3COOH$, pH 3); this mixture was thoroughly mixed and methanol was added to 10 mL. The suspension was centrifuged (6000 rpm × 6 min), the supernatant filtered on 0.45-μm nylon filters (Millex HV, PVDF membrane, 13 mm, Millipore, Vimodrone, Milan, Italy) and 10 μL were injected into the HPLC-DAD apparatus. HPLC-DAD analysis was done according to the method proposed by Hervé et al., with minor modifications [18].

3-PKA was quantified using a calibration curve ($y = 0.0085x + 0.7493$, $R^2 = 0.9998$, constructed by triplicate injections of 3-PKA, purified by semipreparative HPLC [11], from 0.1 μg to 10 μg. The limit of detection (LOD, calculated as $3\sigma/S$, where $\sigma$ indicates the standard deviation of the response and $S$ the sensitivity obtained from the slope of the analytical calibration curve) was 0.01 μg injected, and the limit of quantification (LOQ) 0.03 μg. The recovery range, determined on an acacia honey sample (used as blank since it contains no detectable quinoline alkaloids) spiked with known amounts of 3-PKA (10, 50, 100, 200, 500, 1000 mg/kg) and processed as above, was 97.56–103.65%.

4-QUIN and γ-LACT-4-PKA were determined by comparison of the signal integrals deduced from the $^1$H NMR spectra, following the procedure reported by Bradamante et al., with minor modifications [19]. In view of the chromatographic overlap of KA and γ-LACT-3-PKA, this latter was quantified applying the following equation:

$$C_{\gamma\text{-LACT-3-PKA}} = \frac{C_{3\text{-PKA}}}{\text{MW}_{3\text{-PKA}}} \times \frac{[I_{\text{H-5 3-PKA+H-5}\gamma\text{-LACT-3-PKA}} - I_{\text{H-6 3-PKA}}]}{I_{\text{H-6 3-PKA}}} \times \text{MW}_{\gamma\text{-LACT-3-PKA}}$$

where $C_{3\text{-PKA}}$ is the concentration of 3-PKA determined by HPLC-DAD expressed as mg/kg, $I_{\text{H-5 3-PKA H-6 3-PKA+H-5}\gamma\text{-LACT-3-PKA}}$ is the cumulative integral value of the H-5 NMR signals (centered at 8.15 ppm) from 3-PKA and γ-LACT-3-PKA, and $I_{\text{H-6 3-PKA}}$

is the integral value of H-6 from 3-PKA. $MW_{3\text{-PKA}}$ = 259.28 Da and $MW_{\gamma\text{-LACT-3-PKA}}$ = 240.25 Da. For 3-QUIN determination, $I_{H\text{-}3\,4\text{-QUIN}}$, the integral value of H-3 signal from 4-QUIN ($\delta$ 6.67 (d)) was substituted for $I_{H\text{-}6\,3\text{-PKA}}$ and $MW_{\gamma\text{-LACT-3-PKA}}$ with $MW_{4-\text{QUIN}}$ = 145 Da. The amount of γ-LACT-3-PKA was then subtracted from that of KA, quantified by HPLC (calibration curve 0.1–10 μg; $y = 0.0083x + 0.5431$, $R^2 = 0.9998$; LOD = 0.01 μg injected; LOQ = 0.03 μg; recovery range 96.65–104.3%).

### 2.4. Semipreparative HPLC-DAD

HPLC analysis of honey was done on a Varian LC-940 semipreparative HPLC system (Varian, Turin, Italy) equipped with a binary pump system, an autosampler, a fraction collector, a UV-DAD detector operating at λ = 327 nm and a scale-up module. Analytical separations were carried out using two pursuit XRs 5 C18 columns (250 mm × 4.6 mm and 250 mm × 21.2 mm). Solvent system A = 0.1% TFA in $H_2O$ and B = 0.1% TFA in MeOH. Gradient 0–15 min B = 95%, 15–25 min B = 5%, 25–35 min B = 35%.

### 2.5. HPLC-DAD-ESI-MS analysis

HPLC-DAD-ESI-MS analysis was done with a Thermo Finnigan LCQ Advantage ion trap mass spectrometer (Thermoquest, Milan, Italy) coupled to a Thermoquest Surveyor System (Thermoquest, Milan, Italy), equipped with a quaternary pump, a Surveyor Model 6000 LP UV/vis diode array programmable detector operating between 200 and 400 nm, a Surveyor AS autosampler, a vacuum degasser and Xcalibur Software. Components were separated with a Phenomenex Synergy RP80 A column (150 mm × 2 mm i.d., particle size 4 μm) protected with a Max-RP guard column (4 mm × 2 mm i.d. particle size 4 μm). Gradient elution: 100% solvent A [$H_2O$, 0.1% HCOOH] to 60% B [MeOH, 0.1% HCOOH] in 60 min, followed by re-equilibration. Flow rate 0.2 μL/min. The ESI-MS source was set as follows: capillary temperature 220 °C; spray voltage 4.5 kV; capillary voltage 10 V (positive ion mode) or −3 (negative ion mode); sheath gas flow rate 2 L/min; auxiliary gas flow rate 5 L/min. Spectra were detected in positive and negative ion mode (100–500 $m/z$, 0.5 scan/s). For ESI-MS/MS experiments the relative collision energy was set at 35% (optimized using the LCQ-Xcalibur software), the isolation width at $m/z$ 1, with helium as collision gas.

### 2.6. NMR analysis

All the NMR experiments were done on a Bruker Avance 500 spectrometer ($^1$H base frequency 500.13 MHz) using a 5-mm QNP ($^{13}$C-$^{31}$P-$^{19}$F) Z-GRD probe, equipped with a pulsed gradient unit capable of producing magnetic field pulse gradients, in the $z$-direction, of 53.5 G cm$^{-1}$.

Diffusion-ordered spectroscopy (DOSY) NMR experiments were done using bipolar gradient pulses for diffusion measurements, generated by two spoil gradients [20] at 303 K. The duration of the magnetic field pulse gradient ($\delta$) was optimized to correlate with different diffusion times ($\Delta$), to obtain a mean residual signal from 2% to 5% on the whole spectra, in correspondence with application of 95% of the maximum gradient. Optimized values: $\delta$ = 2 ms, $\Delta$ = 100 ms; the pulse gradients ($g$) were raised from 2% to 95% of the maximum gradient, in a linear ramp mode. 16k data points were acquired in direct dimension and series of 32 spectra (number of gradient increments) in the second dimension; number of scans 24; relaxation delay 1 s; eddy current delay ($Te$) 5 ms.

After Fourier transformation and baseline correction, the diffusion dimension was processed with the Bruker XWIN NMR software package (version 3.1) to obtain a pseudo-2D map in which components with different diffusion coefficients are separated along the diffusion axis (indirect axis).

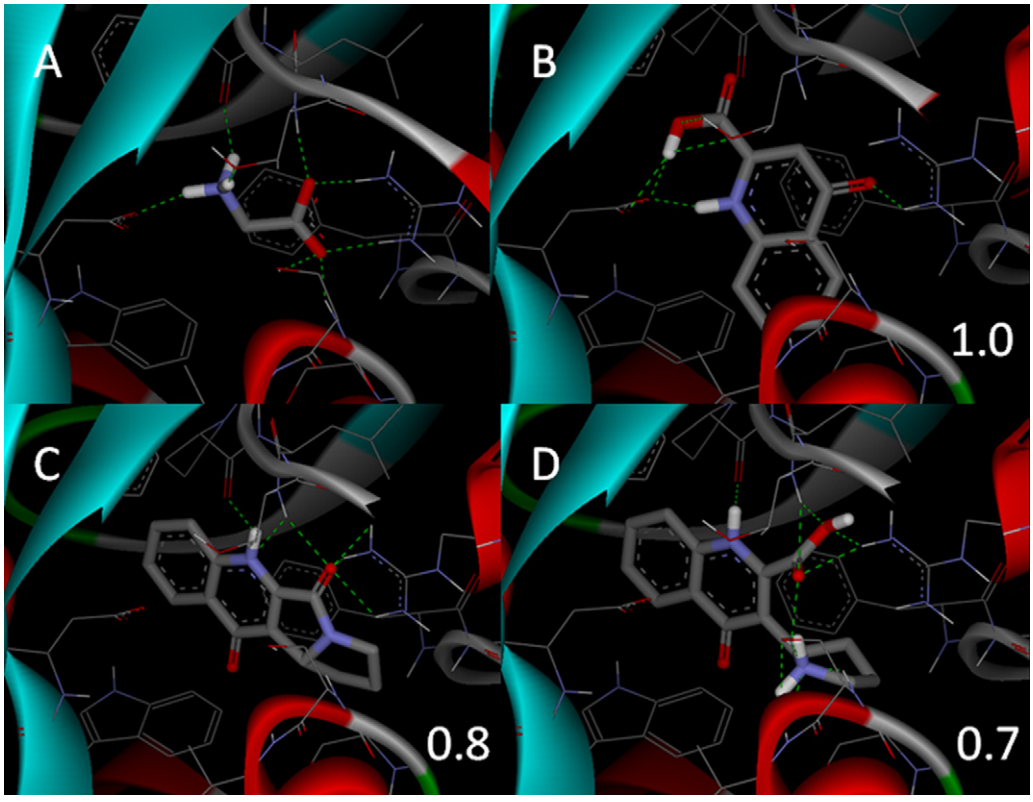


**Fig. 2.** Molecular docking of (A) glycine, (B) KA, (C) γ-LACT-3-PKA and (D) 3-PKA into glycine binding site of the NMDA receptor.

### 2.7. TPC and antiradical activity

TPC and antiradical activity were determined as previously described [15].

### 2.8. Molecular docking

To test the effectiveness of the AutoDock [21] program for studying ligand binding to the NR1 ligand binding core of the NMDA receptor, the glycine molecule was initially docked and the orientation of the resulting lowest energy structure was compared with the crystallographic one. Superposition (RMSD: 0.53 Å) was perfect, demonstrating the AutoDock's ability to locate the glycine binding site.

To find the binding regions of the derivatives in the receptor structure, automated docking simulation was done with the program AutoDock version 3.0. Atomic salvation parameters and fragmental volumes were assigned to the protein atoms using the AutoDock utility, AddSol. All ligand atoms but no protein atoms were allowed to move during the simulation, and the rotatable bonds in the ligand were defined using another AutoDock utility, AutoTors. The interaction energy between ligand and protein was evaluated using atom affinity potentials that are pre-calculated on a grid. A grid map of 7 Å in each *x*, *y*, and *z* direction was used, with a resolution of 0.375 Å, calculated using AutoGrid. Docking was done using the Lamarckian genetic algorithm in AutoDock 3.0. Each docking experiment was run 100 times, yielding 100 docked conformations.

The following parameters were used for docking: population size 50; random starting position and conformation; maximal mutation 2 Å in translation and 50° in rotation; elitism 1; mutation rate 0.02 and crossover rate 0.8; local search rate 0.06. Simulations were done with a maximum of 1.5 million energy evaluations and a maximum of 27,000 generations. The pseudo-Solis and Wets local search method was included with the default parameters. Final docked conformations were clustered with 1 Å RMSD tolerance. Molecular modeling studies were done on a quad-Xeon workstation running Linux.

### 2.9. Multivariate analysis

The distribution of the biomarkers was investigated with multivariate analysis. To identify new, meaningful underlying variables and reduce the size of the data set we did a principal component analysis (PCA), as previously reported, with minor modifications [16]. The results are presented as a score plot. Data Lab 2.593 software (Epina GmbH, Pressbaum, Austria) was used for all calculations.

## 3. Results and discussion

### 3.1. Docking

Crystallographic data retrieved from the Protein Data Bank (entry 1PB7 [22]) contain the NR1 ligand binding core of the NMDA receptor complexed with glycine. The conformations resulting from the docking experiment were clustered and most of them (up to 87%) were located at the glycine binding site of the NMDA receptor. The most important residues forming this binding site (those implicated in hydrogen bond interaction with the ligands) corresponded to $Pro^{124}$, $Thr^{126}$, $Arg^{131}$, $Ser^{180}$, $Val^{181}$ and $Asp^{224}$. The main differences in the binding mode between KA and its two metabolites are depicted in Fig. 2. The carboxylic group of KA points towards the region near the carboxylic group of the $Asp^{224}$ residue, giving rise to four strong hydrogen bonds, three involving the KA carboxylic group and the third the heterocyclic nitrogen (Fig. 2B). The KA heterocyclic moiety is at the center of the binding site, forming an additional H-bond between the keto oxygen of KA and the $Arg^{131}$ residue.

The binding mode of the two derivatives is reversed compared to KA. The heterocyclic moiety in both is oriented towards the $Asp^{224}$ residue, lacking the hydrogen bonds. Both γ-LACT-3-PKA and 3-PKA (Fig. 2C and D) interact with $Pro^{124}$, $Thr^{126}$ and $Arg^{131}$ forming one hydrogen bond with $Pro^{124}$ and two hydrogen bonds both with $Thr^{126}$ and $Arg^{131}$, respectively), while only 3-PKA is able to form three additional H-bonds with $Ser^{180}$ and one with $Val^{181}$ (Fig. 2D). These differences from KA in the binding mode of LACT-PKA and PKA reflect the differences in the calculated affinities (with predicted decreases in affinity of respectively 20% and 30%). However, this theoretical study indicates that both compounds are able to bind to the NMDA receptor, and therefore, by interacting synergistically with KA, potentially contribute *in vivo* to antagonizing the activation of the peripheral NMDA receptor by excitatory amino acids released by injured tissue [14].

These results prompted us in the second part of the study to address the MS characterization of the potentially biologically active KA derivatives, complementary to previous NMR findings [8,11], then to quantify them in honeys of different botanical origins by DOSY NMR and HPLC-DAD.

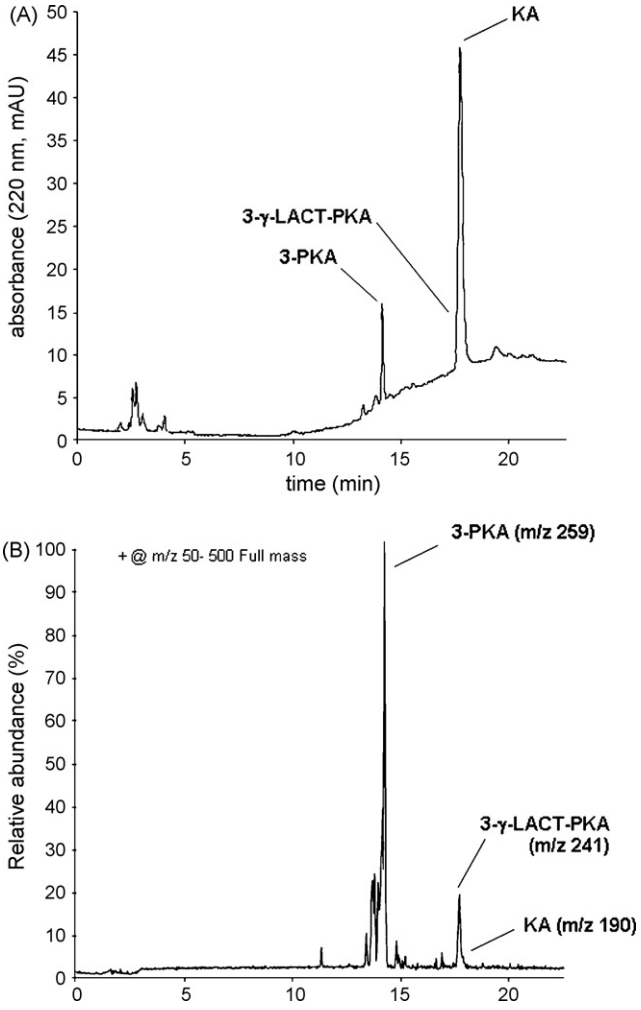


**Fig. 3.** HPLC-DAD-ESI-MS analysis: representative UV-DAD chromatogram at λ = 327 nm (A) and (B) full mass chromatogram of an RP-SPE extract from chestnut honey. KA: kynurenic acid, 3-PKA: 3-pyrrolidinyl-kynurenic acid and γ-LACT-3-PKA: lactam derivative of 3-pyrrolidinyl-kynurenic acid.

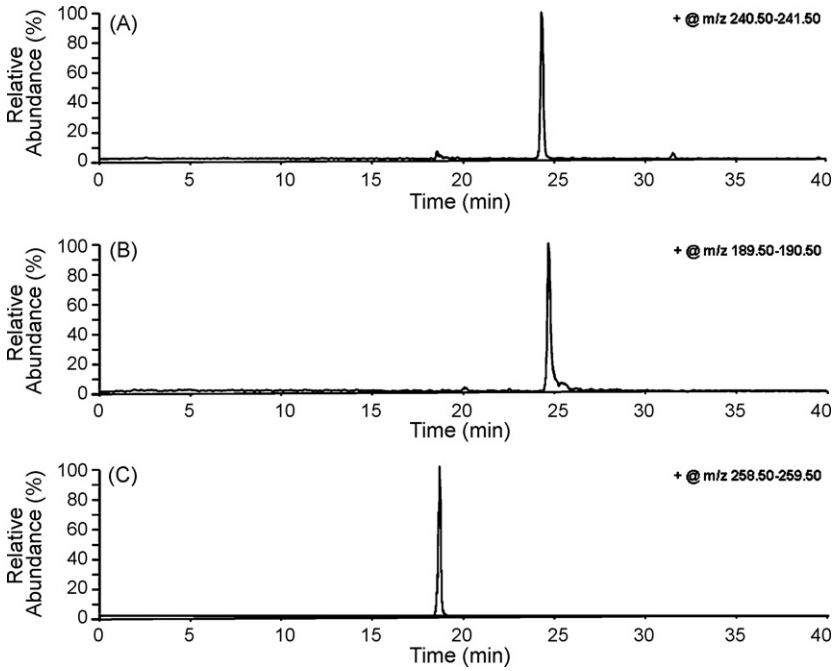


**Fig. 4.** HPLC-ESI-MS chromatograms (positive ion mode, single ion monitoring) of the ions at (A) *m/z* 259 (3-PKA), (B) *m/z* 190 (KA) and (C) *m/z* 231 (γ-LACT-3-PKA).

### *3.2. Mass spectrometric study*

The RP-SPE extract from a chestnut honey (sample 6) was analyzed by HPLC-DAD-ESI-MS and UV (327 nm) and the full mass chromatograms (*m/z* 50–500) are reported in Fig. 3A and B. The two peaks at 18.5 min and 24.0 min showed UV spectral profiles typical of KA and 3-PKA.

3-PKA generated pseudo-molecular ions at *m/z* 259 $[M+H]^+$ in positive ion mode and at *m/z* 257 $[M-H]^-$ in negative ion mode (not shown), corresponding to an even molecular weight of 258 Da and fragments (positive ion mode) at *m/z* 215 $[M\text{-}CO_2+H]^+$ and *m/z* 198 $[M\text{-}CO_2\text{-}NH_3+H]^+$. The elemental composition of these ions, investigated by high-resolution CID mass spectrometric analysis on the $[M+H]^+$ ion detected at 259.10856 ($C_{14}H_{15}N_2O_3$), was consistent with the empirical formulae $C_{13}H_{15}N_2O$ and $C_{13}H_{12}NO$, in accordance with the structure of the 3-pyrrolidinyl derivative of KA (3-PKA, Fig. 1) [11]. Interestingly, 3-PKA generated the most abundant pseudo-molecular ion in positive ion mode, in apparent contrast to the UV trace where KA was the main compound. This difference is explained by the easily protonable secondary amine of its pyrrolidinyl moiety, which causes 3-PKA to respond more strongly than KA to the ESI ionization.

The MS analysis detected a small amount of a third species, almost co-eluting with KA, detectable in the UV trace as a small

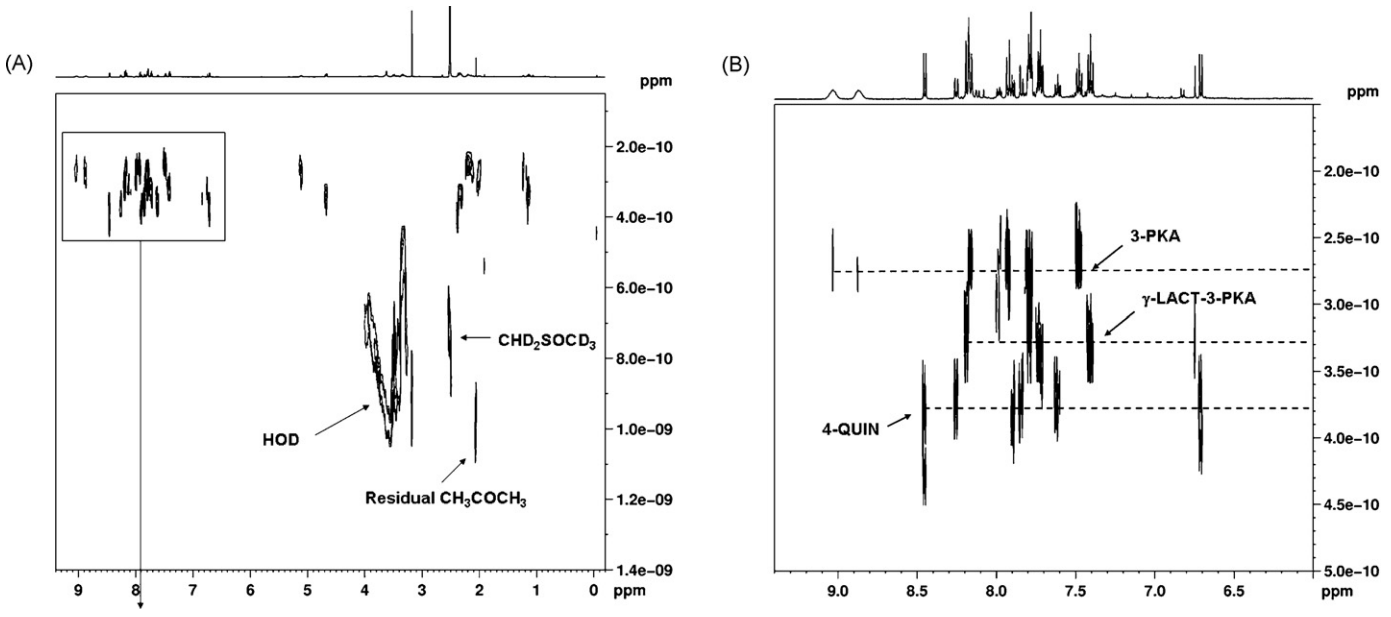


**Fig. 5.** (A) DOSY NMR map of the RP-SPE extract from chestnut honey (sample 7). The axes (*x*, *y*) of the map represent chemical shifts in ppm and diffusion coefficient as Log (value), respectively, and (B) expansion of the aromatic region (6.0–9.5 ppm). Dotted lines indicate relevant compounds: 3-PKA, γ-LACT-3-PKA and 4-ONE-QUIN.

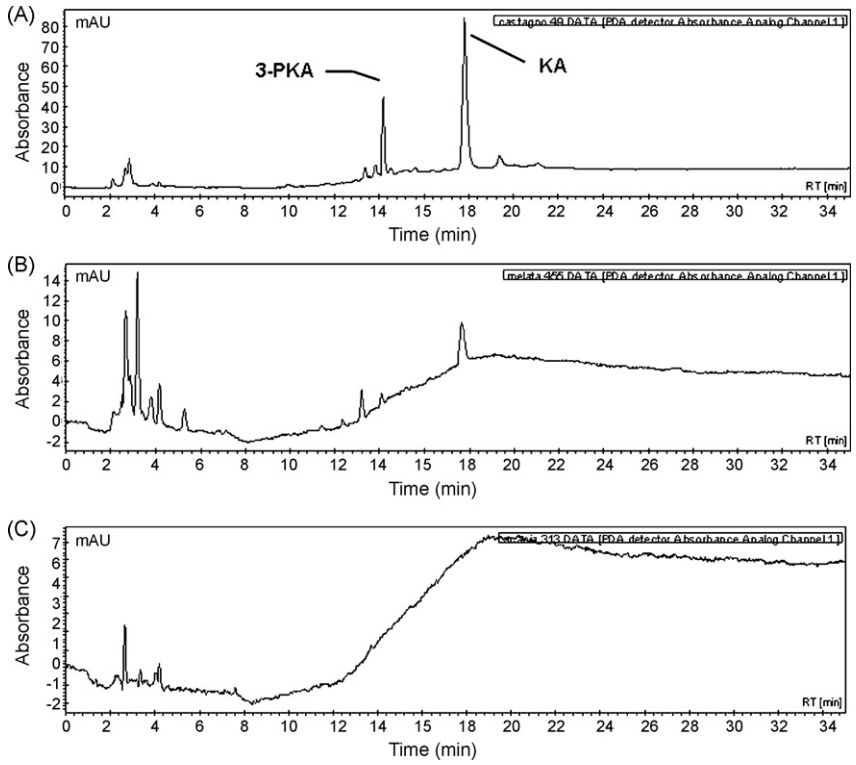


**Fig. 6.** HPLC profile (λ = 327 nm) of (a) chestnut honey, (b) honeydew honey and (c) acacia honey.

left shoulder in the KA peak, predominant and barely resolved in the mass TIC chromatogram, but sharply separated when analyzed in SIM mode (Fig. 4). This was identified as γ-LACT-3-PKA (Fig. 1) [11] on the basis of its pseudo-molecular ions at *m*/*z* 241 $[M+H]^+$ and *m*/*z* 239 $[M-H]^-$ in positive and negative ion modes. Structural assignment was confirmed by CID HR-MS on the pseudo-molecular ion at *m*/*z* 241.10856, which showed neutral losses of $H_2C_2$ from its condensed pyrrolidinyl group, and $C_3H_3N$ from the KA moiety.

### 3.3. DOSY NMR

To obtain further information on other unknown alkaloids as biomarkers of botanical origin, poorly responsive to ESI-MS ionization and/or requiring time-consuming purification, we used DOSY NMR analysis for screening. This allows the separation of the individual NMR spectral components of mixtures, and their identification with no need for physical separation [23], since this technique uses the molecular diffusion rate in solution to separate resonances generated by different compounds in a mixture [24,25]. Fig. 5a shows a representative DOSY spectrum of the RP-SPE extract from the sample of chestnut honey (sample no. 8), which had the lowest content of KA and the highest of 3-PKA and γ-LACT-PKA.

Starting from lower to higher diffusion coefficients, by analysis of the map we first identified the solvents (HOD, $CD_2HSOCD_3$, residual methanol and acetone), then at higher diffusion coefficients (Fig. 5b), the resonances of 3-PKA and of γ-LACT-3-PKA (see above), and of an additional species at δ 6.7 (d), δ 7.6 (t), δ 7.85 (d), δ 7.9 (t), δ 8.25 (d), δ 8.45 (d). In the light of these $^1$H NMR data, and its lower diffusion coefficient (which indicates a smaller molecular size than 3-PKA and γ-LACT-3-PKA) this last species was preliminarily identified as 4-quinolone (4-QUIN, MS studies are in progress), a compound already shown to have antimicrobial activity [26], which may arise from the metabolization of kynuramine or 5-hydroxy-kynuramine by monoamine oxidase (MAO) intervention in the plant or in the honeybee [3,27].

### 3.4. Quantitative analysis of quinoline alkaloids

We analyzed 24 samples of commercial honey of 15 different botanical origins by HPLC-DAD for the quantitative determination of KA ($\lambda_{max}$ = 332 nm). Since 3-PKA was not commercially available, it was determined after isolation from chestnut honey by semipreparative HPLC, setting the acquisition wavelength at $\lambda_{max}$ = 327 nm.

In view of the chromatographic overlap of KA and γ-LACT-3-PKA peaks, we quantified them with the aid of $^1$H NMR integral values, as described in the Section 2. This allows the precise determination of γ-LACT-3-PKA (and of the previously unidentified 4-QUIN) with a significant saving of the time required for the difficult and expensive gradient elution approach needed to separate γ-LACT-3-PKA and from KA.

Fig. 6 reports the representative UV chromatographic profiles of honeys from chestnut (panel A), honeydew (B), and acacia (C) monitored at 220 nm. In chestnut honey the KA and 3-PKA peaks were easily detectable. In honeydew honey the concentrations were lower, with 3-PKA barely detectable, and were undetectable in acacia honey.

The concentrations of KA and of 3-PKA are reported in Table 1. In accordance with the semi-quantitative determination of KA reported in previous papers [8,28], HPLC indicated a higher content of KA in chestnut honey (from 701 to 2114.9 mg/kg) than in the other honeys from arboreal species such as honeydew, almond, and eucalyptus, while 3-PKA was 10–20 times lower than KA, except in sample 7, where KA was significantly lower than in samples 1–6, with parallel increases of 3-PKA and γ-LACT-3-PKA (Table 1).

Among the honeys from arboreal species, only those from acacia, orange and *Tilia* (lime) had no detectable amounts of any quinoline alkaloid though exceptions were samples 9, 10, 13 and 14, which contained small amounts of KA (<200 mg/kg), probably due to contamination from chestnut honey [28]). These observations suggest there is some chestnut-specific honeybee feeding material (from chestnut flower nectar or sugar-rich tree exudate) containing the

**Table 1**
Content of KA, 3-PKA, 3-γ-LACT-PKA and 4-QUIN, total phenol content ($mg_{GAE}$/kg, TPC) and antiradical activity (ARA; $mg_{GAE}$/kg ARA) in 24 different honey samples. n.d. = not detectable. Data are reported as mg/kg.

| | Honey type | KA | 4-PKA | 3-γ-LACT-PKA[a] | 4-QUIN | TPC | ARA |
|---|---|---|---|---|---|---|---|
| 1 | Chestnut | 2114.9 ± 73.4 | 482.8 ± 17.5 | n.d. | n.d. | 696.6 ± 35.1 | 651 ± 14 |
| 2 | Chestnut | 1885.1 ± 46.5 | 206.9 ± 9.4 | n.d. | n.d. | 727.0 ± 27.5 | 570 ± 17 |
| 3 | Chestnut | 1643.7 ± 13.8 | 218.4 ± 6.9 | n.d. | n.d. | 641.4 ± 23.4 | 710 ± 32 |
| 4 | Chestnut | 1172.4 ± 25.4 | 114.9 ± 4.7 | n.d. | n.d. | 880.9 ± 33.5 | 623 ± 16 |
| 5 | Chestnut | 1069.0 ± 35.8 | 160.9 ± 5.8 | n.d. | n.d. | 801.4 ± 36.8 | 637 ± 13 |
| 6 | Chestnut | 701.1 ± 10.1 | 80.5 ± 3.4 | n.d. | n.d. | 859.2 ± 41.3 | 684 ± 17 |
| 7 | Chestnut | 680.3 ± 8.3 | 80.5 ± 3.4 | n.d. | n.d. | 715.1 ± 32.5 | 722 ± 36 |
| 8 | Chestnut | 23.1 ± 2.6 | 643.8 ± 15.4 | 845.8 ± 11.7 | 743.4 ± 20.7 | 791.8 ± 41.4 | 751 ± 31 |
| 9 | Honeydew | 126.4 ± 4.6 | n.d. | n.d. | n.d. | 847.7 ± 27.3 | 460 ± 21 |
| 10 | Sunflower | 125.3 ± 4.9 | 23.0 ± 1.6 | n.d. | n.d. | 495.0 ± 18.4 | 303 ± 14 |
| 11 | Acacia 1 | n.d. | n.d. | n.d. | n.d. | 194.9 ± 12.6 | 90 ± 4 |
| 12 | Acacia 2 | n.d. | n.d. | n.d. | n.d. | 233.5 ± 11.4 | 150 ± 8 |
| 13 | Acacia 3 | 23.1 ± 1.6 | n.d. | n.d. | n.d. | 202.4 ± 14.5 | 123 ± 6 |
| 14 | Multiflora | 103.4 ± 4.1 | n.d. | n.d. | n.d. | 324.6 ± 19.4 | 126 ± 7 |
| 15 | Almond | 92.5 ± 3.6 | 11.5 ± 0.5 | n.d. | n.d. | 776.0 ± 33.8 | 182 ± 9 |
| 16 | Eucalyptus | 143.4 ± 6.7 | n.d. | n.d. | n.d. | 518.7 ± 25.2 | 235 ± 13 |
| 17 | Heather | n.d. | n.d. | n.d. | n.d. | 1200.4 ± 55.2 | 740 ± 29 |
| 18 | Linden | n.d. | n.d. | n.d. | n.d. | 391.6 ± 23.5 | 230 ± 16 |
| 19 | Sulla | n.d. | n.d. | n.d. | n.d. | 283.0 ± 15.2 | 181 ± 25 |
| 20 | Thymus | n.d. | n.d. | n.d. | n.d. | 1636.3 ± 61.3 | 940 ± 29 |
| 21 | Lavender | n.d. | n.d. | n.d. | n.d. | 421.1 ± 21.5 | 430 ± 18 |
| 22 | Dandelion | n.d. | n.d. | n.d. | n.d. | 381.3 ± 16.9 | 310 ± 16 |
| 23 | Rosemary | n.d. | n.d. | n.d. | n.d. | 277.6 ± 14.3 | 417 ± 26 |
| 24 | R. mosqueta | n.d. | n.d. | n.d. | n.d. | 614.5 ± 34.3 | 61 ± 4 |

[a] Calculated from $^1$H NMR signal integrals.

quinoline alkaloids (basically KA and 4-PKA) that are absent in all the other botanical varieties. In this context, γ-LACT-3-PKA can be considered a simple rearrangement product arising from non-enzymatic intramolecular condensation between the C2 carboxyl moiety of 3-PKA and the aminic nitrogen of its pyrrolidinyl side chain, a reaction that can occur during honey storage or heating.

In agreement with a previous report [8,16,28], all the other honeys from herbal flowers (dandelion, lavender, thyme, French honeysuckle [*Hedysarum coronarium*], heather, cardoon, *Rosa mosqueta* and rosemary) had no detectable quinoline alkaloids.

### 3.5. TPC and TAA

Table 1 reports the TPC and TAA of the honeys. TPC values were within the ranges reported in the literature [15] and significantly higher in dark varieties (thyme, chestnut and heather) than pale ones (acacia, rosemary). The TAA showed a similar pattern, in accordance with its strong correlation with TPC reported by several authors.

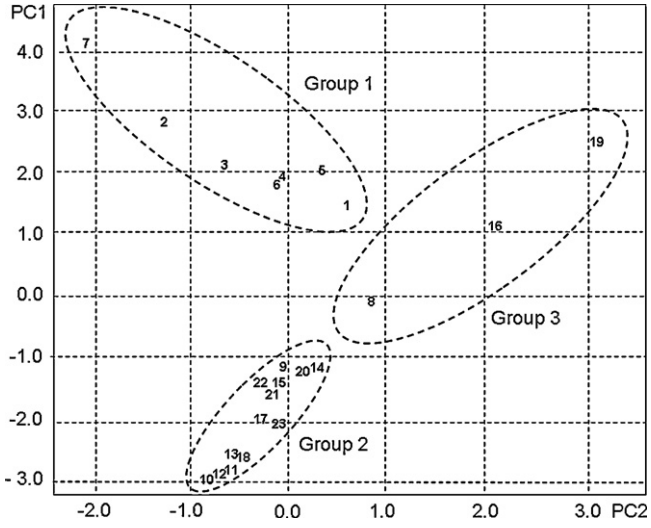


**Fig. 7.** Score plot from PCA.

### 3.6. Chemometric analysis

In order to distinguish the potential uses of honey of different botanical origins for dermatological and nutritional purposes, we

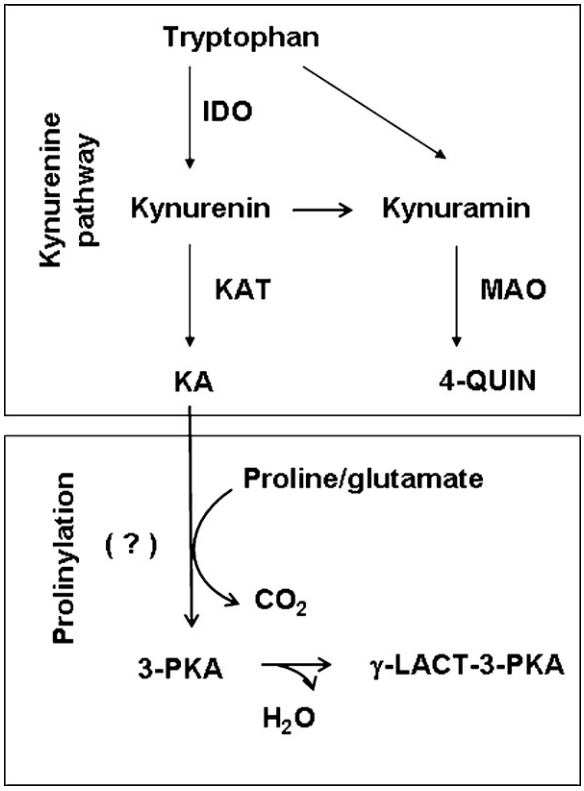


**Fig. 8.** Schematic representation of the kynurenine pathway and proposed 3-PKA biosynthetic mechanism.

did PCA on: (i) the content of the major quinoline alkaloids (KA and 3-PKA); (ii) total phenol content (TPC) and (iii) antiradical activity (DPPH), reported in Table 1.

Fig. 7 reports the PCA score plot. Along PC1, honeys were separated mainly on the basis of their quinoline alkaloid content, while TPC and TAA were the main variables in PC2. Samples were clustered in three definite groups with chestnut honeys in group 1 (samples 1–7), separated from all the others. Most of the others were clustered in group 2 in the lower left side of the plot, with the exception of samples 8 (honeydew honey), 16 (heather honey), and 19 (thyme), which were assigned to group 3 on account of their higher antiradical activities than those in group 2.

## 4. Conclusions

The results of this study provide two sets of information. The first regards the composition of honeys of different botanical origins, and shows that chestnut honey is rich in quinoline alkaloids with potential antinociceptive activity while herbal honeys contain antiradical constituents with potential antiinflammatory activity. These activities interact with the well-known peroxide-dependent antibacterial action present in all honeys, from different sources [29] and help heal topical lesions. This information based on the qualitative/quantitative profiling of these pharmaco-active principles might explain the efficacy of honey in the treatment and resolution of specific dermatological lesions (burns, wounds, diabetic ulcers, etc.) resistant to conventional therapies.

The second set of information relates to the possible metabolic interplay between quinoline alkaloids in chestnut honey, which can be considered an extension of the kynurenine pathway. Through a combination of different MS and NMR techniques, we have demonstrated that among various honeys from different botanical origins chestnut honey has the highest content of the quinoline alkaloids KA, 3-PKA, γ-LACT-3-PKA, 4-QUIN. Interestingly, in most samples of chestnut honey KA was predominant, in others virtually only its derivatives, thus supporting the idea of metabolic conversion between KA and 3-PKA, γ-LACT-3-PKA and 4-QUIN.

These may play a role in the honeybee's tryptophan metabolism: after the intervention of indoleamine-2,3-dioxygenase (IDO) on kynurenine for KA biosynthesis (this latter has a marked action in honeybee neuro-activity [3]), its turnover can be influenced by the enzymatic formation of pyrrolidinyl metabolites according to the scheme reported in Fig. 8 [27].

Further studies are needed to elucidate the mechanism underlying this different distribution, very likely involving the kynurenine pathway and proline or its precursor glutamate, which are found in the honeybee's intestinal microflora. The presence of these metabolites and their biopharmaceutical and physiological roles (KA elimination, storage, turnover, modulation, etc.) in insects, microorganisms, plants and mammals are currently under investigation.

## References

[1] J. Liebig, Justus Liebigs Ann. Chem. 86 (1853) 125–126.
[2] F. Moroni, P. Russi, G. Lombardi, M. Beni, V. Carlà, J. Neurochem. 51 (1988) 177–180.
[3] V.B. Smirnov, E.G. Chesnokova, N.G. Lopatina, E. Voike, Neurosci. Behav. Physiol. 36 (2006) 213–216.
[4] A.N. Starratt, S. Caveney, Phytochemistry 42 (1996) 1477–1478.
[5] D. Kuc, M. Rahnama, T. Tomaszewsky, W. Rzeski, K. Wejksza, T. Urbanik-Sypniewska, J. Parada-Turska, M. Wielosz, W.A. Turski, Amino Acids 58 (2006) 393–398.
[6] D. Kuc, W. Zgrajka, J. Parada-Turska, T. Urbanik-Sypniewska, W.A. Tursky, Amino Acids 35 (2008) 503–505.
[7] M.P. Turski, M. Turska, W. Zgrajka, D. Kuc, W. Turski, Amino Acids 36 (2008) 75–80.
[8] G. Beretta, E. Caneva, R. Maffei Facino, Planta Med. 73 (2007) 1592–1595.
[9] M.N. Perkins, T.W. Stoner, Brain Res. 247 (1982) 184–187.
[10] C. Prescott, A.M. Weeks, K.J. Staley, K.M. Partin, Neurosci. Lett. 402 (2006) 108–112.
[11] G. Beretta, G. Vistoli, E. Caneva, C. Anselmi, R. Maffei Facino, Magn. Res. Chem. 47 (2009) 456–459.
[12] P.C. Molan, Int. J. Low Extrem. Wounds 5 (2006) 40–54.
[13] J.S. Gòmez-Jeria, L. Lagos-Arancibia, Int. J. Quantum Chem. 71 (1999) 505–511.
[14] B.E. Cairns, G. Gambarota, P.S. Dunning, R.V. Mulkern, C.B. Berde, Pain 98 (2003) 521–529.
[15] A. Tonks, R.A. Cooper, A.J. Price, P.C. Molan, K.P. Jones, Cytokine 14 (2001) 240–242.
[16] G. Beretta, P. Granata, M. Ferrero, M. Orioli, R. Maffei Facino, Anal. Chim. Acta 533 (2005) 185–191.
[17] G. Beretta, E. Caneva, L. Regazzoni, N. Golbamaki Bakhtiari, R. Maffei Facino, Anal. Chim. Acta 620 (2008) 176–182.
[18] C. Hervé, P. Beyne, H. Jamault, E. Delacoux, J. Chromatogr. B 675 (1996) 157–161.
[19] S. Bradamante, L. Barenghi, G. Beretta, M. Bonfà, M. Rollini, M. Manzoni, Biotechnol. Bioeng. 80 (2002) 589–593.
[20] D. Wu, A. Chen, C.S. Johnson, J. Magn. Reson. A 115 (1995) 260–264.
[21] G.M. Morris, D.S. Goodsell, R.S. Halliday, R. Huey, W.E. Hart, R.K. Belew, A.J. Olson, J. Comput. Chem. 19 (1998) 1639–1662.
[22] http://www.rcsb.org.
[23] P.A. Keifer, Curr. Opin. Biotechnol. 10 (1999) 34–41.
[24] C.S. Johnson, Prog. Nucl. Magn. Res. Spectrosc. 34 (1999) 203–256.
[25] K.F. Morris, C.S. Johnson, J. Am. Chem. Soc. 115 (1993) 4291–4299.
[26] T.P. Cushnie, A.J. Lamb, Phytomedicine 13 (2006) 187–191.
[27] T.W. Stone, L.G. Darlington, Nat. Rev. Drug Discov. 1 (2002) 609–620.
[28] J.A. Donarski, S.A. Jones, M. Harrison, M. Driffield, A.J. Charlton, Food Chem., doi:10.1016/foodchem.2008.10.033, in press.
[29] A.I. Schepartz, M.H. Subers, Biochim. Biophys. Acta 85 (1964) 228–237.